Temporal and Spatial Variations of Precipitation and Temperature in the Yongding River Basin under the Influence of Climate Change, 1959–2020

Hui Gwang Yun [1,*], Il Chol Kim[a] Kwang Jin Rim[1], Chol Ho Chae[1]

[1]Faculty of Geoscience and Technology, Kim Chaek University of Technology, Pyongyang, 999093 Democratic People's Republic of Korea

*** Corresponding Author**

DOI : https://doi.org/10.51584/IJRIAS.2025.10100000152

Received: 23 October 2025; Accepted: 30 October 2025; Published: 18 November 2025

ABSTRACT

Global climate change has a considerable impact on the temporal and spatial fluctuations of precipitation. The Yongding River basin (YRB) temperature and precipitation variations in inter-annual and inter-seasonal scales were determined by analyzing daily temperature and precipitation data of 53 meteorological stations from 1959–2020.

The Mann-Kendall test (MK), spearman's correlation analysis, and moving t-test (MTT) were used to examine the temporal variation and spatial distribution of precipitation. The results indicated the annual mean temperature at all 53 stations has significantly increased with the highest located in the Guanting Reservoir and around Langfang City. The annual precipitation changes showed a decreasing trend at 25 stations of Beijing, Tianjin, and Langfang city, while an increasing trend at the other 28 stations of Datong, Shuozhou, and Zhangjiakou city. However, there was not a single station that showed a significant increase or decrease.

The correlation analysis between annual temperature and precipitation in the YRB revealed that, 86% of stations showed a negative correlation. The MTT method (N1 = N2 = 10) identified temperature jumps in 1986-1998 and 2010-2011, while the MK method detected jumps in 1992 and 2015-2017. Analysis of the annual series data revealed that 12.9% of the YRB experienced three temperature jumps, 71.07% had one jump, and 16.03% had no jumps, while average annual precipitation jumps, 73.87% of the watershed area had a single jump, 26.13% had two jumps, and no area remained unaffected.

These findings indicate that changes in summer and autumn precipitation, exhibiting high variability and severity, are the primary drivers of annual precipitation jumps in the YRB. All these data can be used to develop sensible regulatory and management policies for the basin's water resources, ensuring the health of the many ecosystems that make up the region.

Keywords: precipitation, temperature, temporal and spatial variation, climate change, climate jump

INTRODUCTION

Climate change has emerged as one of the most pressing environmental issues of the 21st century, attracting elevated attention from the international community as well as national governments [1]. The average global temperature increased by 0.85 °C between 1988 and 2012, at a rate of 0.064 °C per decade according to Intergovernmental Panel on Climate Change's Fifth Report, such an increase in global temperature would suffice to influence regional hydrological cycles, including changes in the spatial and temporal distribution of precipitation [2]. Global warming could aggravate the unequal distribution of precipitation, resulting in more rain in wet places and less rain in dry ones [3,4]. While, the concept of "arid areas becoming drier and humid areas increasing wetter" does not apply to all places, only about 11% of worldwide precipitation over land has been "drier and wetter" since 1948 [5], and extreme precipitation events are anticipated to become more intense and frequent in specific sections of the mid-latitudes and humid tropics [2].

China's average climate, as well as the features of extreme weather and climate events, has changed as a result of global warming [6]. Since 1960, China's average temperature has increased by 1.2 °C [7]. The extreme weather and climate events have varied in frequency, severity, timing, length, and spatial extent as a result of climate change, and reports of record-breaking extreme events occurrences have been progressively increasing [8,9]. Many scholars have compared observations and models to look at the trends in precipitation extremes in China. The results reveal a rising frequency of extreme precipitation occurrences and increased **precipitation** on a national basis, but regional-scale results are more diverse [10].

Some researcher studied daily precipitation data of the Haihe River basin from 1960 to 2010, one of China's seven largest river basins with the worst water scarcity, and found that precipitation in this river basin was on the declining trend[11,12]. Annual precipitation in the Haihe River basin decreased with an average slope of -0.57 mm a^{-2} from 1959 to 2016 by evaluating data from 57 sites in this river basin [13]. Precipitation in plain areas of the Haihe river basin was higher than that in mountainous and hilly areas [14]. Yu et al presented pertinent findings on the evolution of precipitation in the Haihe River basin, reporting a gradual decline from east to west and south to north[15].

The Yongding River is the largest branch of the Haihe River basin and is also called Beijing's mother river [16], and has suffered from many disasters. According to historical records, in the 800 years before the founding of the People's Republic of China (new China) in 1949, the Yongding River breached, overflowed, and changed course 149 times. Under the influence of climate and land surface changes, the surface runoff in the Yongding River mountainous area has gradually decreased, and the natural runoff has decreased from 1.971 billion m^3 before the 1970s to 839 million m3 from 2001 to 2014. Since the 1960s, different degrees of drying up and depletion happened in the Yongding River's lower reach, especially after 1980, with the increase in industrial, agricultural, and municipal water usage, the river flow downstream of Lugou Bridge was cut off for 197 days in the 1960s, 361 days in the 1980s, and the whole year in the 1990s. The river completely dried up with the river bed exposed, and the groundwater level in the surrounding area continued to decline. At the same time, the rapid economic and social development leads to the over-exploitation of water resources in the basin and the water quality in most reaches of the river has been deteriorating for a long time. For example, the Guanting reservoir, situated in the Yongding River, is the first large reservoir built after the founding of new China and was once of Beijing's main water supply sources. As the reservoir's water quality deteriorated, it was forced to withdraw from the city's drinking water system in 1997 [17].

Since 2000, the State Council of China has approved and implemented the Plan for Sustainable Utilization of Water Resources in the Capital in the early twenty-first century and the Plan for Water Allocation in the main stream of the Yongding River to alleviate the scarcity of water resources in Beijing, rationally allocate water resources in the basin, ensure the safety of water supply in the Capital to ensure sound, rapid economic and social development in the basin. In the upper reaches of the Guanting reservoir, key projects such as agricultural water-saving, soil erosion control, point source pollution control, industrial water-saving, and urban sewage treatment plant construction have been carried out, and centralized water supply to the Guanting reservoir has achieved remarkable results, with significantly increased water intake and improved water quality[18]. However, the dry situation of the lower reaches of the Yongding River has not been improved. The rivers downstream of the Lugou Bridge dried up all year round, which could not guarantee the water demand of the ecological environment and caused serious ecological degradation in the water-scarce area associated with the Yongding River [19,20]. It has seriously harmed the river's ecological function and hampered the long-term economic and social development of the coordinated development zone of Beijing, Tianjin, and Hebei [21].

The response of hydrological processes to precipitation changes and climate variabilities, as well as the resulting changes in regional water conservation capacity, are critical for the sustainable use of water resources. Due to the fact that a detailed analysis of the climate variability of all seasons, including temperature and precipitation, as well as their interrelationship, has not been performed for the Yongding River basin, this study aims (i) to investigate seasonal and annual variabilities in precipitation and temperature in the basin; and (ii) to detect climate jumps and precipitation periodicities over a 62-year climatological period from 1959 to 2020. It allows a comprehensive review of the seasonal climatology and trends in precipitation and temperature in the Yongding River basin, which may be of exemplary significance internationally to study such a basin.

METHODOLOGY

Study Area

Physical geography

The Yongding River Basin, as shown in Fig. 1, is located between 112°00'~117° 45' E and 39°00'~41°20' N. The Yongding River basin covers an area of 47,053 km^2, of which the mountain area covers 45,100 km^2, accounting for 95.8%, and the plain area covers 1,953 km^2, accounting for 4.2% [22].

River system

Yongding River, one of the four major national flood control channels in China, flows through Inner Mongolia autonomous regions, Shanxi province, Hebei province, Beijing, and Tianjin City, and belongs to the northern system of the Haihe River basin, as shown in Fig. 1. Yongding River upstream consists of two tributaries, Yanhe River from the Inner Mongolia Plateau and Sanggan River from the Shanxi Plateau. The two rivers flow through alternate ravines valleys, and basins and merge at Huailai Zhuguantun, and after the confluence, they are called the Yongding River. At Guanting the Yongding River is joined by the Guishui River, goes through the Guanting Gorge, and at Sanjiadian into the plain. From Sanjiadian both sides of the Yongding River are constrained by the embankment. There is the Xiaoqing River diversion channel after Lugou Bridge. After Lianggezhuang the Yongding River enters its flooded area and is joined by the Tiantang River and Longhe River. At Qujiadian it is called the Yongding New River after the outlet of the flooded area. After Dazhangzhuang, the Yongding new river takes in the Beijing sewage river, Jinzhong River, Chaobai New River and Jiyunhe River to flow into the sea at Beitang, Tianjin City. Among the rivers, the Sanggan River is the main source of the Yongding River, 390 km long, the Yanghe River is 101 km long, the Yongding River is 307 km long, the Yongding New River is 62 km long, and a total length of the Yongding River is 761 km.

Hydrometeorology

The Yongding River basin is a temperate continental monsoon climate, which is a climate transition zone between semi-humid and semi-arid. The spring dries early with some sandstorms, summer is hot with heavy rains, autumn is cool with little rainfall, and winter is cold and dry. The annual average temperature is 6.9 ℃, the highest 39℃ and the lowest -35℃. The frost-free period in the basin area is 120-170 days and about 100 days in the mountainous area, and the frozen period is more than 4 months. The average annual precipitation in the Yongding river basin ranges from 360 mm to 650 mm, and there is a large difference in precipitation in different areas, and the difference between the rainy and dry areas is nearly doubled. The annual variation of precipitation is large, with a difference of 2-3 times between dry years and rainy years, and precipitation in flood season (June to September) accounts for 70% to 80% of the total year. The annual average runoff of the Yongding River Basin area from 1956 to 2010 was 1.443 billion m^3, which was unevenly distributed within the year and varied greatly in different years. The maximum annual runoff that emerged in 1956 was 3.14 billion m^3, the minimum annual runoff in 2007 was 672 million m^3, and the ratio of maximum annual runoff to minimum annual runoff was 4.67.

Economy and society

The administrative division of the Yongding River Basin includes parts of Beijing, Tianjin, Hebei, Shanxi, and Inner Mongolia with 51 cities, counties, and districts, among which Hebei province involves three prefecture-level cities of Zhangjiakou, Baoding, Langfang, and Shanxi Province involves three prefecture-level cities of Xinzhou, Shuozhou, and Datong[20].

From 2017 to 2020, the resident population of 8 major cities or districts (Shuozhou and Datong in Shanxi, Zhangjiakou, and Langfang in Hebei, Yanqing District, Mentougou District, Fangshan District and Daxing District in Beijing) in the Yongding River Basin has increased from about 17.81 million in 2017 to 18.33 million in 2020. The growth rate was higher than the growth rate of the permanent population in the four provinces (cities) of Beijing, Tianjin, Hebei, and Shanxi during the same period. From 2017 to 2019, the per capita GDP

ISSN No. 2454-6194 | DOI: 10.51584/IJRIAS |Volume X Issue X October 2025

of the eight cities (districts) in the basin increased from 45,900 yuan in 2017 to 51,700 yuan in 2019, up 12.6%[21].

The mountainous area upstream of the Yongding River is rich in mineral resources and is an important energy base and renewable energy demonstration area in China, as well as an important food and vegetable producing area in the region. The central part is the southwest gateway of China's Capital, Beijing. It is densely populated and has a high urbanization rate. It will be a cluster area for the development of the high-end service industry, technology industry, and modern manufacturing industry in the future. Tianjin Binhai New Area of the downstream, located in the coastal region, boasts an advanced manufacturing industry, modern service industry, scientific, technological innovation, research and development base. It will be the future shipping and logistics centre of northern China and an important economic development belt of the Beijing-Tianjin-Hebei region[22].

Figure 1. The study area and metrological stations map.

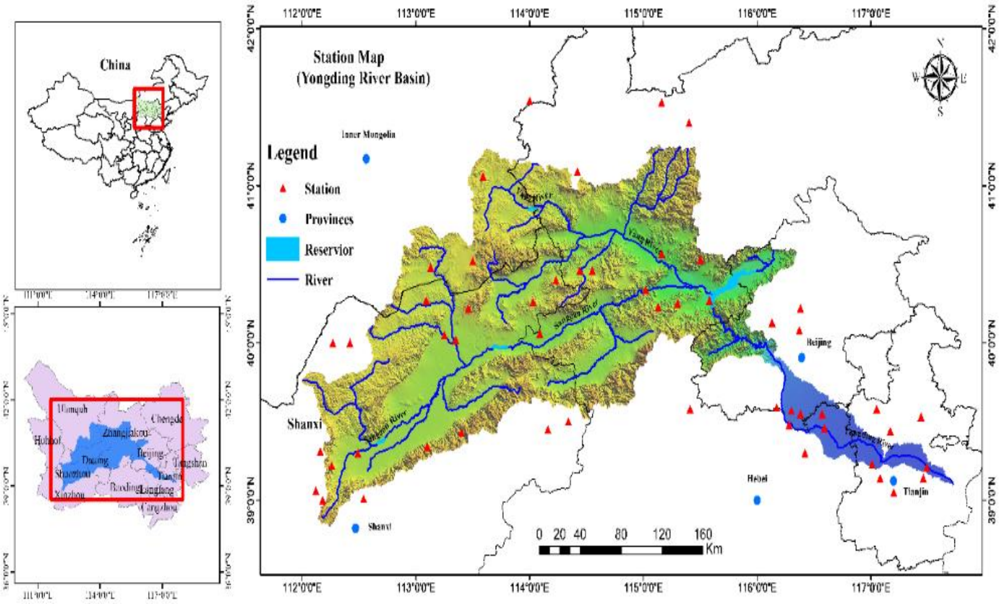

Data and Method

Data

Daily precipitation and temperature from the China Meteorological Administration (CMA) were collected in 53 meteorological stations located throughout the Yongding River Basin from January 1959 to December 2020 for this study, as shown in Figure 1, while monthly and annual data were derived from daily data. The 62-year data set of 53 meteorological stations was deemed long enough to draw reliable climatic conclusions and reveal the true state of temporal precipitation changes in the Yongding River Basin.

Method

In this study, we utilized the Thiessen polygon method to estimate the area-mean temperature and precipitation. Additionally, we employed the Mann-Kendall trend test and the Kriging interpolation method to investigate the spatial variation of precipitation and temperature during the period from 1959 to 2020.

A two-tailed t-test with a confidence level of 95% was used to test the null hypothesis slope using a linear fitted model. This method is commonly employed for statistical diagnosis in modern climatic analysis. We also used a linear fitted model and a two-tailed t-test with a confidence level of 95% to examine the temporal variation of precipitation and temperature throughout the 1959–2020 period.

Spearman's correlation analysis was applied to determine the correlations between the mean temperature and mean precipitation on an annual and seasonal basis.

To identify jumps in temperature and precipitation on an annual and seasonal scale, we employed the non-parametric Mann-Kendall change point test and the moving t-test. These tests were utilized for temporal analysis.

Furthermore, we utilized the Kriging interpolation method to create spatial distribution maps depicting significant changes and jumps in temperature and precipitation, as well as correlations between temperature and precipitation, within the Yongding River Basin.

The Thiessen polygon method

Thiessen Polygon, also known as the Thiessen Method or Voronoi Diagram, is indeed a widely used technique for evaluating area mean precipitation quantity or area mean temperature. Proposed by climatology expert Alfred Thiessen in 1911, this method involves creating polygons by connecting points on a plane with their nearest observation point. These Thiessen polygons are utilized extensively in climate-related research[23,24].

The use of Thiessen polygons offers a fast, simple, and reasonably accurate way to calculate rainfall and temperature. The technique only requires information such as the precipitation and temperature values at each station, as well as the calculated station weight or area of influence (referred to as Thiessen Constant or Area Factor). By considering these factors, the method allows for the estimation of area mean values based on the available data.

This approach has proven useful in various climatological studies and is often employed in research involving climate analysis, hydrology, and meteorology. The Thiessen Polygon technique provides a spatial representation of the data, taking into account the proximity of observation points, which helps in understanding the distribution and patterns of precipitation or temperature across an area [25]

After the application of this formula, the mean precipitation or temperature of each polygon is calculated by multiplying the precipitation or temperature value of polygons with the weighted mean [26]. The mean precipitation or temperature of the entire study area is calculated using the following formula after finding the mean precipitation or temperature of all polygons:

Thiessen method is simply described as:

$$W_i = \frac{A_p}{A}$$

(1)

W_i: weighted area of Thiessen polygons

A_P: The area of Thiessen polygons

A: Total study area

$$P = \sum_{i=1}^{n} W_i P_i \qquad (2)$$

P: The areal mean precipitation or temperature of the study area

P_i: Precipitations or temperatures of meteorological stations within Thiessen polygons

n: Number of total Thiessen polygons

Average areal precipitation and temperature were estimated by Thiessen polygon method using ArcGIS software [27].

The Mann–Kendall Trend Test

The higher the auto-correlation in the time series, the greater the error when using the Mann-Kendall test [28]. Given the time series {xi, i = 1, 2, ..., n}, the auto-correlation in time series must be removed generally according to the following procedure [29].

At first,

ISSN No. 2454-6194 | DOI: 10.51584/IJRIAS |Volume X Issue X October 2025

$$\rho_1=\frac{Cov(x_i, x_{i+1})}{Var(x_i)}=\frac{\frac{1}{n-2}\sum_{i=1}^{n-1}(x_i-\bar{x})(x_{i+1}-\bar{x})}{\frac{1}{n-1}\sum_{i=1}^{n}(x_i-\bar{x})^2} \quad (3)$$

where ρ_1 is first order auto-correlation coefficient, $Cov(x_i, x_{i+1})$ is the covariance between the variables x_i and x_{i+1} and $Var(x_i)$ is the variance of x_i.$\bar{x}$ is arithmetic mean of series x.

Then, remove the auto-correlation from the original time series:

$$x_i'=x_i-\rho_1 x_{i-1} \quad (4)$$

If i=1 then $x_0 = 0$.

Simply, the transferred series $\{x_i', i = 1,2,...,n\}$, is still noted as $\{x_i, i = 1,2,...,n\}$, calculate Kendall indicator, τ, variance, σ_τ^2, standard deviation, σ_τ, as well as normalized variable U [28].

$$\tau=\frac{4p}{n(n-1)}-1 \quad (5)$$

Where

$$p=\sum_{k=1}^{i} n_k \quad (6)$$

Where n_k is the number of later records in the series whose values exceed x_i.

$$\sigma_\tau^2=\frac{2(2n+5)}{9n(n-1)} \quad (7)$$

$$U=\tau/\sigma_\tau \quad (8)$$

U is used to reflect the trend in hydrological or meteorological time series, The larger the |U|, the more obvious the changing trend, and if U > 0, the trend is increasing, and vice versa.

Given the significance level α, the standard normal-distribution table can be used to calculate the critical value $U_{\alpha/2}$; if $|U| > U_{\alpha/2}$, reject the hypothesis of no trend and assume the changing trend is significant. For example, given α = 0.05, then, $U_{\alpha/2} = U_{0.025} = 1.96$.

Spearman's Correlation Analysis

The Spearman's correlation coefficient is a nonparametric index used to measure the dependence between two variables. This method, which does not require data distribution information and can better reflect the correlation between precipitation and temperature, uses a monotone equation to evaluate the correlation between two statistical variables [22].

It is calculated as:

$$\rho=1-\frac{6\sum_{i=1}^{n} d_i^2}{n(n^2-1)} \quad (9)$$

Where ρ = the Spearman's correlation coefficient, d_i = the difference between the ranks of corresponding variables, and n = the number of observations.

Therefore, the degree of correlation between the two variables was determined using the ρ-values (ρ∈ [-1,1]), and its degree classification standards are shown in Table 1 [30].

Table 1 Classification standards of Spearman's correlation

Degree of Correlation	Correlation Coefficient Value
Completely uncorrelated	$\lvert\rho\rvert = 0$
Weak correlation	$0.01 \le \lvert\rho\rvert \le 0.19$

Low correlation	$0.20 \leq \lvert\rho\rvert \leq 0.39$
Moderate correlation	$0.40 \leq \lvert\rho\rvert \leq 0.59$
Significant correlation	$0.60 \leq \lvert\rho\rvert \leq 0.79$
High correlation	$0.80 \leq \lvert\rho\rvert \leq 0.99$
Strong correlation	$\lvert\rho\rvert = 1$

Moving t-Test

The moving t-test (MTT) detects climate jumps in a series by comparing the significant differences between the averages of two groups of samples. In China, this strategy is commonly utilized to detect climatic jump occurrences [31,32]. The subsequence X_1 of the N_1 samples was acquired before the datum point with an average of $\overline{X_1}$ and a variation of S_1^2, and the subsequence X_2 of the N_2 samples was obtained after the datum point with an average of $\overline{X_2}$ and a variance of S_2^2 [33]. The t-statistic is written as follows:

$$t=\frac{\overline{X_1}-\overline{X_2}}{\sqrt{\frac{N_1S_1^2+N_2S_2^2}{N_1+N_2-2}\left(\frac{1}{N_1}+\frac{1}{N_2}\right)}} \quad (10)$$

Given a significance level of α, the null hypothesis of no differences will be rejected if $|t| > t_{\alpha/2}$. Climate jump places can be affected by the length of the subsequence set. To overcome this, two conditions were used: $N_1=N_2=5$ and $N_1=N_2=10$. A 95% confidence level was used as a standard. The time scope of the climate leap was defined by all locations satisfying $|t| > t_{\alpha/2}$ after the statistic was calculated, and climate leaps may occur in years when |t| reaches maximum. The t-statistic with a significance level of α is $t_{\alpha/2}$, of 5% for this study.

Mann-Kendall Change Point Test

The test statistic S_k is defined as follows:

$$S_k=\sum_{i=1}^{k}\sum_{j=1}^{i-1}\alpha_{ij} \quad (k=2, 3, 4, \cdots, n) \quad (11)$$

$$\alpha_{ij}=\begin{cases}1 & x_i>x_j \\ 0 & x_i\leq x_j\end{cases} \quad 1 \leq j \leq i \quad (12)$$

and the statistic index UF_k is defined as follows: $UF_k=\frac{S_k-E(S_k)}{\sqrt{Var(S_k)}}$

k=1, 2, 3, 4, ⋯, n(13)

where:

$$E(S_k)=\frac{k(k-1)}{4} \quad (14)$$

$$Var(S_k)=\frac{k(k-1)(2k+5)}{72} \quad (15)$$

The same equation is used to calculate a backward sequence UB_k, but with a reversed series of data. If there was a point of intersection between the two curves (UF_k and UB_k), that point would be considered the change point [34].

RESULTS AND DISCUSSIONS

Spatial and Temporal Analysis of Temperature

Spatial Analysis of Temperature Change

Figure 2 illustrates the spatial distribution of significant levels of the annual and seasonal mean temperature variations in the Yongding River Basin. The Mann–Kendall test involving annual mean temperature data during the 1959–2020 period at all 53 stations showed an increasing trend, with the increasing trend being significant

ISSN No. 2454-6194 | DOI: 10.51584/IJRIAS |Volume X Issue X October 2025

at all stations (Figure 2a). Specifically, the most intense increase in temperature is observed in the eastern regions including Zhangjiakou, Beijing, and Langfang, and the gentlest in Datong city, which showed a spatial difference.

The mean temperature of each season in all areas of Yongding River Basin from 1959 to 2020 tended to increase (Fig. 2b, c, d, e). The increasing trend of the mean spring, and summer temperature was significant in all areas, especially in Zhangjiakou and Langfang city for the mean spring temperature, and in Langfang City for the mean summer temperature. Except for most parts of Datong City and a small part of Beijing and Tianjin, the increasing trend of mean autumn temperature in the study area is significant. For the mean winter temperature, except for most area of Datong City, all other areas showed an increasing trend.

Figure 2. Spatial distribution of the significance of annual and seasonal mean temperatures (a) annual; (b) spring; (c) summer; (d) autumn, and (e) winter.

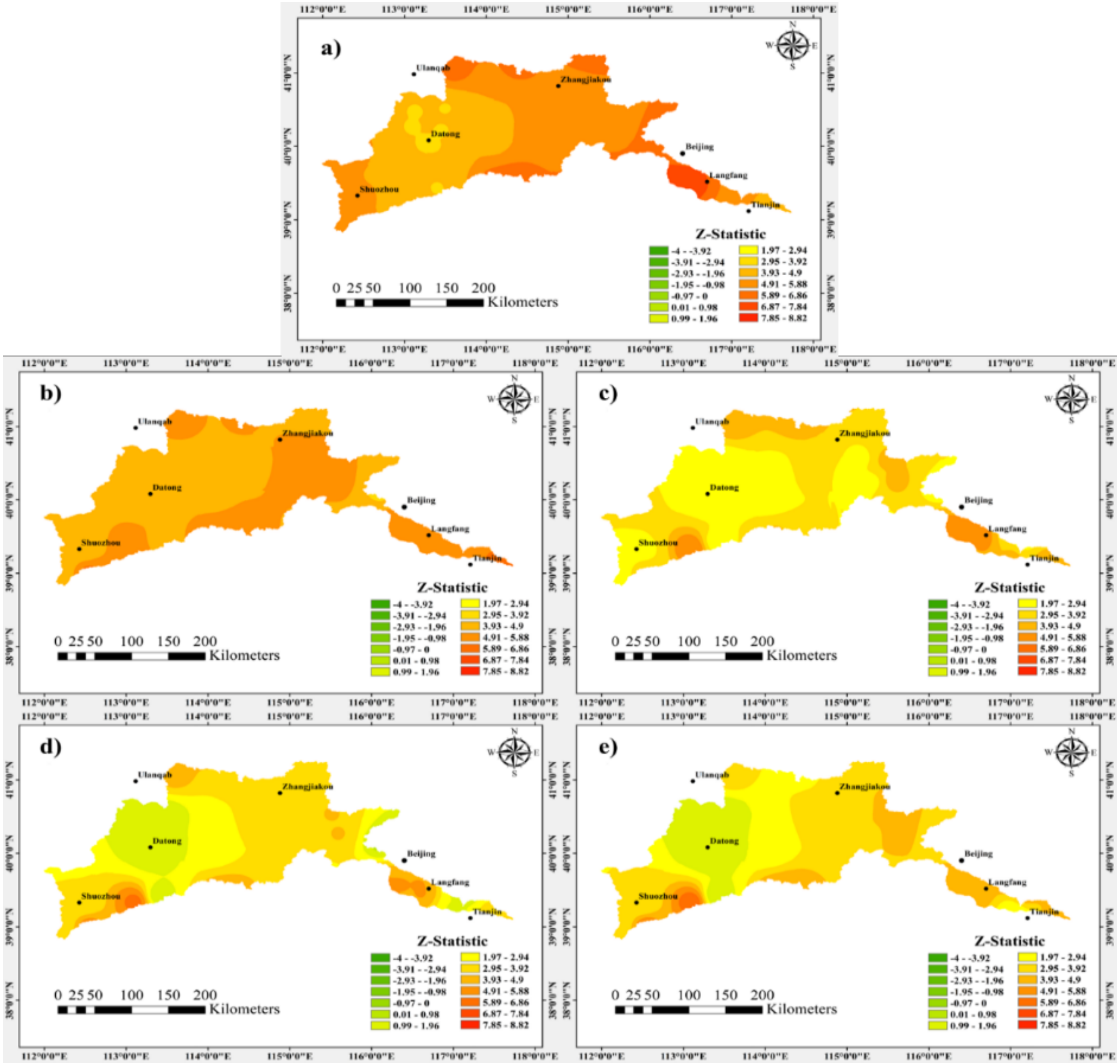

Temporal Analysis of Temperature Change

In order to get the temporal trend of seasonal and annual mean temperatures, the area-integrated method of temperature by dividing Thiessen polygons is used to obtain the area's seasonal and annual mean temperatures from 1959 to 2020, as shown in Figure 3.

As a whole, the basin's temperature increases at a rate of around 0.38°C/10 a, 0.22°C/10 a, 0.2°C/10 a, 0.38°C/10 a, and 0. 29°C/10a respectively in the spring, summer, autumn, and winter season, and annually, which are significant at the 5% level of significance.

ISSN No. 2454-6194 | DOI: 10.51584/IJRIAS |Volume X Issue X October 2025

Figure 2. Spatial distribution of the significance of annual and seasonal mean temperatures (a) annual; (b) spring; (c) summer; (d) autumn, and (e) winter.

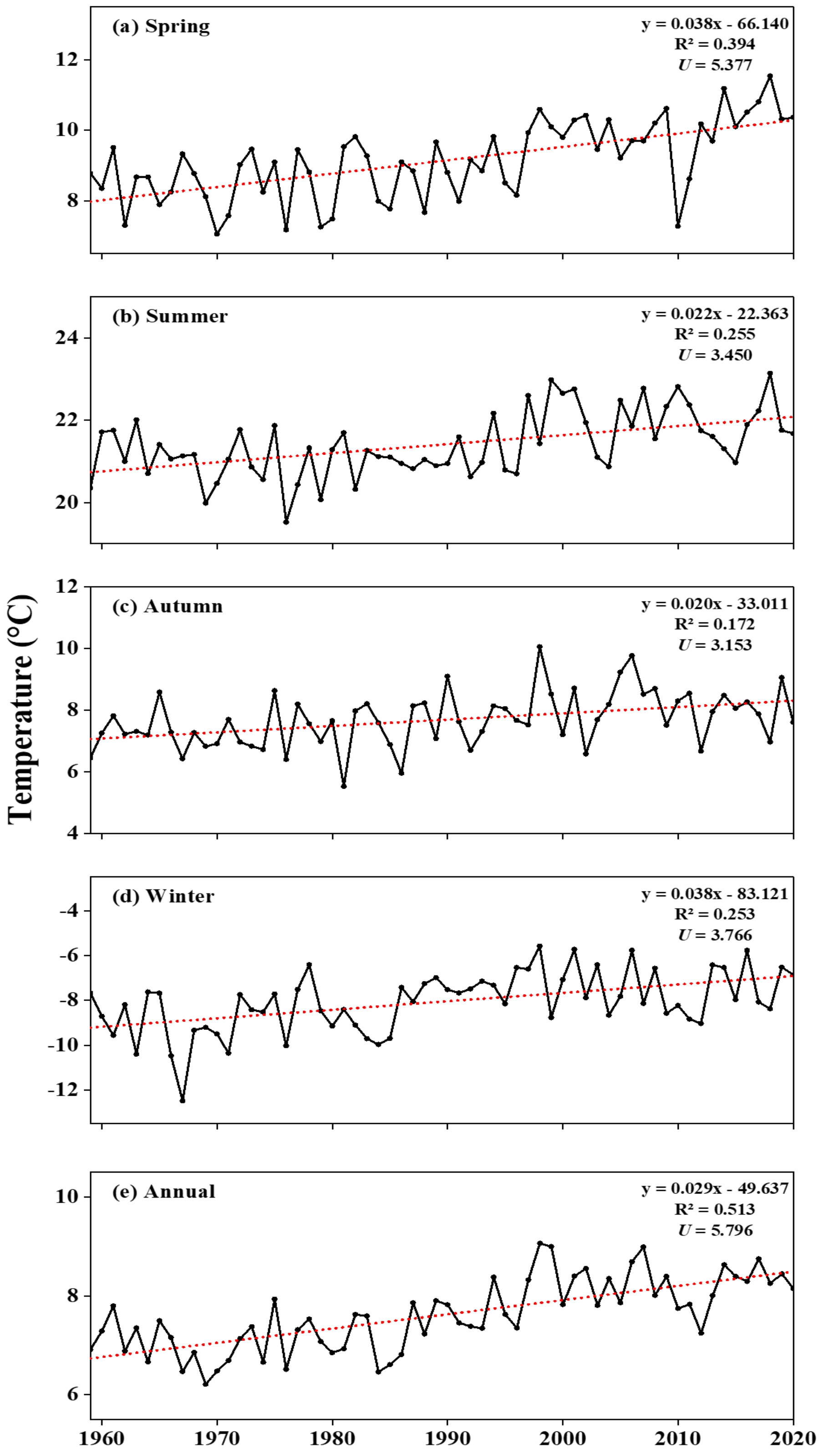

Spatial and Temporal Variability of Precipitation

Spatial Variability of Precipitation

The Mann–Kendall test was carried out to determine the precipitation trend for annual and seasonal variations of precipitation in the Yongding River Basin from 1959–2020. The spatial distribution of the significant levels of yearly and seasonal mean precipitation variation was depicted in Figure 4.

Figure 4: Spatial distribution of the significance of annual and seasonal mean precipitation variations (a) annual; (b) spring; (c) summer; (d) autumn, and (e) winter.

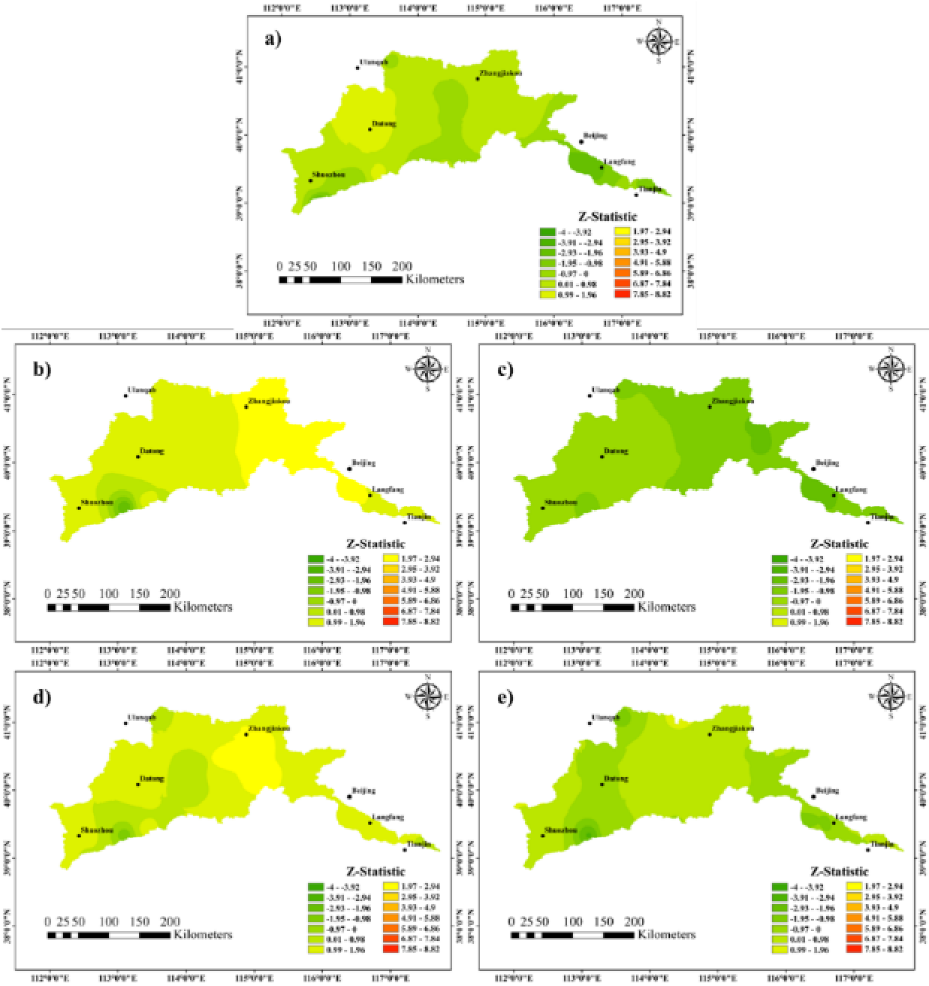

Annual precipitation in the eastern Yongding River Basin, including the areas downstream of Guanting Reservoir and the southern section of Shuozhou City, showed a falling tendency, whereas annual precipitation in the western half of the basin showed a not significantly increasing trend (Figure 4a). Except for a few areas in Shuozhou City, the Yongding River Basin's spring precipitation trended upward, with significant changes in Zhangjiakou City and Beijing (Figure 4b). A decreasing trend in summer precipitation in the Yongding River Basin was found with the trend in the eastern regions of Zhangjiakou City being significant (Figure 4c). Autumn precipitation exhibited a growing trend across the river basin, with the increase being significant in the majority of Zhangjiakou City's regions, except for a few parts in Shuozhou City (Figure 4d). Except for the western and central regions of Shuozhou City and Datong City, the river basin showed a declining trend in winter precipitation (Figure 4e).

In terms of the annual precipitation trend at the 53 hydrological stations of the Yongding River Basin, as shown in Table 2, like 25 stations (i.e., 47.2% of all stations) showed a decreasing trend in annual precipitation without a single station is being significant, while the other 28 stations (i.e., 52.8% of all stations) showed an increasing trend without any being significant station.

Table 2. Annual and seasonal precipitation trends in the Yongding River Basin

Season	Increasing Trend			Decreasing Trend		
	Number of Stations	Percentage (%)	Number of Significant Changes	Number of Stations	Percentage (%)	Number of Significant Changes
Annual	28	52.8	0	25	47.2	0
Spring	53	100	13	0	0	0
Summer	0	0	0	53	100	13

ISSN No. 2454-6194 | DOI: 10.51584/IJRIAS |Volume X Issue X October 2025

Autumn	53	100	5	0	0	0
Winter	23	43.4	0	30	56.6	0

At all 53 locations, a tendency toward decreasing summer precipitation and an increase in autumn precipitation have been seen, with the former trend being significant at 13 stations and the latter in 5 stations. Winter precipitation in the Yongding River Basin is generally low compared to summer precipitation, hence decreases in summer precipitation led to decreases in annual precipitation. Summer and winter are the rainiest seasons in the region.

Temporal Variability of Precipitation

The thiessen polygon method is employed to obtain the seasonal and annual mean precipitation for 53 weather stations from 1959 to 2020. Following this, the temporal trends of the seasonal and annual area-averaged precipitation are calculated, as shown in (Figure 5).

Figure 5: Temporal trend of the area-average precipitation in Yongding River basin from 1959 to 2020: a) spring; b) summer; c) autumn; d) winter; e) annual.

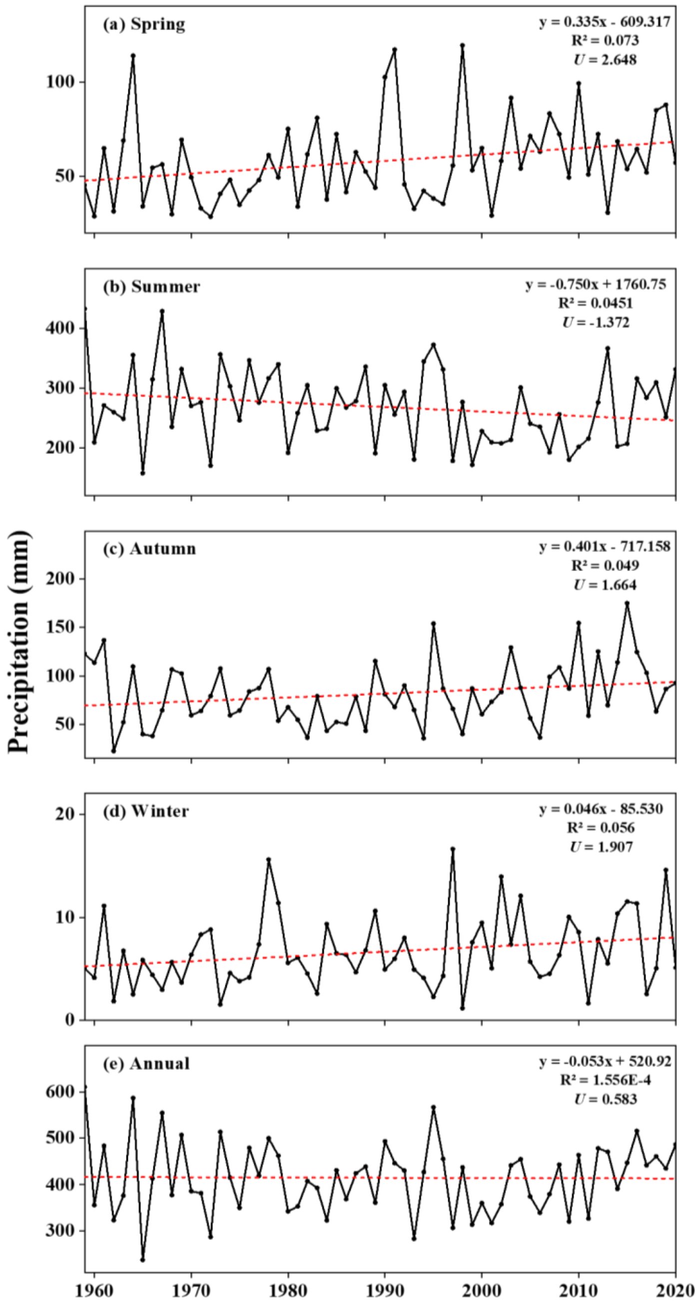

In the spring season (Figure 5a), precipitation increased at a rate of around 3.35mm/10a, which is not significant at the 5% significance level. In the summer season, precipitation decreased at a rate of around 7.5mm/10a, which is significant at the 5% level of significance (Figure 5b). The precipitation in the autumn season was increasing at the rate of around 4.01mm/10a, and the increasing trend in precipitation is not significant at the 5% level of significance. In the winter season (Figure 5d), the precipitation was increasing at a rate of about 0.46mm/10a, which is not significant at the 5% level of significance. Annual precipitation (Figure 5e) were decreased at a rate of 0.53 mm/10a, and this trend is not significant at a 5% level of significance.

The Yongding River basin had an average annual precipitation of 473 mm from 1959 to 2020, with variations over the 62 years ranging from 299 to 718 mm and a variation coefficient of 0.189. The difference between the highest and lowest yearly precipitation was almost 2.4 times. Precipitation in the summer, which has a mean value of 316 mm and makes up 66.7% of the yearly total, reflects the fluctuation in annual precipitation as shown in Figure 5b, e. Both annual and summer precipitation rates decreased during the study period, with a trend of -0.053 mm a-2 and -0.75 mm season-1 a-1, respectively (Figure 5b, e). The ratio of summer precipitation to yearly precipitation stayed essentially stable between 1959 and 2020; the patterns for the two periods are remarkably similar. This is a result of a decline in precipitation, which mainly occurred in the summer.

Spearman's Correlation Analysis Results

The ρ-values belonging to each station were analyzed and calculated in order to assess the degree of association between precipitation and temperature at both the inter-annual and inter-seasonal scales. The findings of grade analysis conducted after correlation coefficient determination are displayed in Table 3.

Table 3. Distribution of statistics for the ρ-values corresponding to different numbers of stations in the Yongding River Basin.

ρ-Value Range	Nature	Spring		Summer		Autumn		Winter		Inter-annual Correlation	
		(+)	(-)	(+)	(-)	(+)	(-)	(+)	(-)	Positive	Negative
0	Completely non-correlations	1	1	0	0	4	4	2	2	0	2
0.01–0.19	Weak correlations	36	13	0	7	12	30	24	21	7	33
0.2–0.39	Low correlations	2	0	0	20	2	1	0	4	0	11
0.4–0.59	Moderate correlations	0	0	0	24	0	0	0	0	0	0
0.6–0.79	Significant correlations	0	0	0	2	0	0	0	0	0	0
0.8–0.99	Highly correlated	0	0	0	0	0	0	0	0	0	0
1	Completely correlated	0	0	0	0	0	0	0	0	0	0

Analysis of the Correlation between Annual Mean Temperature and Annual Precipitation

46 stations in the Yongding River Basin (or 86.8% of all the stations selected) showed negative correlations between annual mean temperature and annual precipitation, as indicated in Table 3, with 33 and 11 stations displaying weak and low negative correlations, respectively. In contrast, 7 stations (or 13.2% of all the stations selected) showed positive correlations, with all of the 7 stations being weak positive correlations. Furthermore, just 2 stations, or 3.8% of the total, exhibited no relationships. The yearly mean temperature and annual precipitation generally correlated negatively in the Yongding River Basin.

ISSN No. 2454-6194 | DOI: 10.51584/IJRIAS |Volume X Issue X October 2025

Figure 6 depicts the regional distribution of Spearman's correlation coefficients at the seasonal and interannual scales. The Yongding River Basin has a relatively concentrated distribution of the correlations and a generally negative correlation between annual mean temperature and annual precipitation. However, the central sections of the basin showed only a faint negative correlation, while some part of the west region of the basin showed only a weak positive correlation.

Figure 6: Spatial distribution of Spearman correlation coefficients in seasonal and inter-annual scale, (a) annual; (b) spring; (c) summer; (d) autumn, and (e) winter.

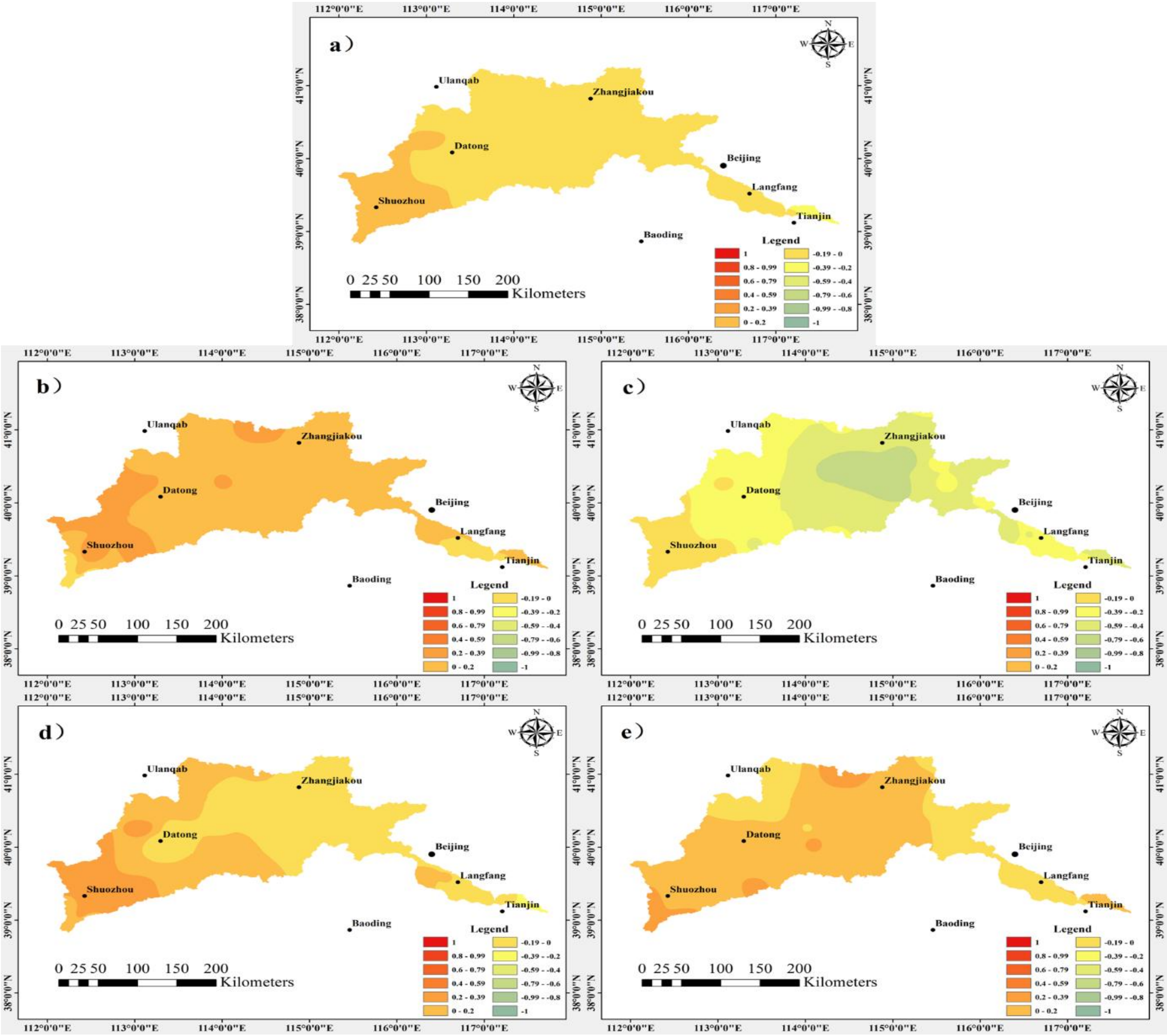

Analysis of the Correlation between Mean Temperature and Precipitation for Different Seasons

In the Yongding River Basin, mean temperatures and precipitation were shown to be negatively correlated during the spring, summer, autumn, and winter seasons (Figure 6). In particular, 13 stations (or 24.5% of all stations) showed weak negative correlations during the spring season. Contrarily, 38 stations (71.7% of the total number of stations) exhibited positive correlations, with 36 and 2 stations indicating weak and low positive correlations, respectively, while 2 stations (3.8% of the total number of stations) indicated an atypical association between temperature and precipitation. In summer, negative correlations were observed at 53 stations (i.e., 100% of the total number of stations), with 7, 20, 24, and 2 stations showing weak, low, moderate, and significant negative correlations, respectively.

In the autumn season, 14 stations (or 26.4% of all stations) displayed positive correlations, with 12 and 2 stations exhibiting weak and low positive correlations, respectively. In contrast, negative correlations were seen at 31 stations (or 58.5% of the total number of stations), with 30 and 1 station exhibiting weak and low negative correlations, respectively. In this season, there were 8 stations (or 15.1% of all the stations) that indicated no association between temperature and precipitation. In the winter, there were 25 stations with negative correlations (i.e., 47.2% of the total number of stations), with 21 and 4 of those stations displaying weak, low correlations. In this season, there were 4 stations (or 7.5% of the total number of stations) that exhibited no correlation whereas 24 stations (or 45.3% of the total number of stations) displayed positive correlations, all of which were weak correlations.

In terms of spatial distribution, although there was an overall negative association between mean temperature and precipitation for different seasons in the Yongding River Basin, the Spearman's correlation coefficients for each of these seasons were noticeably different. In particular, in the spring, the majority of the Yongding River Basin's regions showed a weak positive correlation, while the southwest and southeast small regions showed a weak negative correlation; in the summer, the entire Yongding River Basin showed a negative correlation, and a moderate negative correlation was only observed in the central regions; in the autumn, the central and eastern regions showed a low negative correlation, the west region showed weak and negative correlations. The regions with weak positive associations were sporadically dispersed.

Analysis of Climate Jumps

It is necessary to analyze and comprehend the change and process of the climate system using nonlinear theories and methods because the climate system is a nonlinear and discontinuous phenomenon. Examples of such nonlinear theories and methods include the theory of abrupt changes and the detection method [35]. Many researchers have studied regional climate characteristics on different time scales in China over the last few decades. The findings provided a solid foundation and direction for precisely grasping large-scale climate characteristics and better understanding regional climate change [12].

In this study, 62 years' worthy data of climate trends for climate variables collected from 53 gauging stations in the Yongding River Basin detected at the 95% level of significance. The Yongding River Basin climate change study was separated into investigations on temperature and precipitation changes. The MTT method was used for climate jump detection, and detection results may vary depending on the length selection of the subsequence. Consequently, it makes sense to combine other methods when using the MTT method. We applied MTT and MK mutation test methods for the two parameters. The assessment of significant differences between the averages of two groups of samples necessitates the use of sub-sequences of more than one length in climatic jump detection. The length of the subsequence is adopted as N1=N2=5 and N1=N2=10 as to the comparison period in this study, considering the length of the resulting series. The results generated by both methods are not always consistent since climate leaps discovered by the MK method indicate a major shift in trends whereas climate jumps found by the MTT method show a considerable difference between the averages of the two-subsequence series [32].

Temperature and Precipitation Climate Jumps Temporal variation

The seasonal and annual precipitation was analyzed by the M-K test method and Moving T-test. Figure 7 showed the MTT and MK tests used to find climate jumps in seasonal temperature from 1959 to 2020 in Yongding River Basin.

In the period from 1959 to 1981, the mean temperature in spring exhibited a decreasing trend, while in 1982 to 2020, it displayed an increasing tendency. In the periods of 1999–2020, the tendency is significant as the normalized variable exceeds the confidence level. The climate jump in mean temperature occurred in spring 1997.

The average summer temperature first increases then decrease and then increases again, but overall, it shows an increasing trend. From 1959 to 1968, the average summer temperature showed an increasing trend, while in 1969 to 1998, it shows a decreasing trend, and 1999 to 2020, it shows an increasing trend again. For the period 2007-2020, the trend is significant as the normalized variable exceeds the confidence level. The average climate jump in summer temperature occurred in 1997.

The average autumn temperature experiences a process of decreasing first, followed by an increase, but it shows an overall increasing trend. In the period from 1959 to 1968, the mean autumn temperature exhibited an increasing trend. From 1969 to 1982, it displayed a decreasing tendency, while in 1983 to 2020, it again showed an increasing trend. Furthermore, in the periods of 1999 and 2004–2020, the tendency is significant as the normalized variable exceeds the confidence level. The climate jump in mean autumn temperature occurred in 1988-1989.

In the period from 1959 to 1976, the mean temperature in winter exhibited a decreasing trend., while in 1977 to 2020, it displayed an increasing tendency. In the periods of 1992–2020, the tendency is significant as the normalized variable exceeds the confidence level. The climate jump in mean temperature occurred in winter 1986.

As shown in the above results, the temperature jumps were presented in all seasons. The results can be showed that temperature jumps occurred in all seasons, although the years in which the jumps occurred differed slightly between the two calculation methods. For example, in autumn, the MTT method showed two climatic jumps in 2004 and 2009 and the MK method showed one climatic jump in 1988-1989.

Figure 7. Moving t-test (a-d) and Mann-Kendall mutation test (e-h) of seasonal temperature.

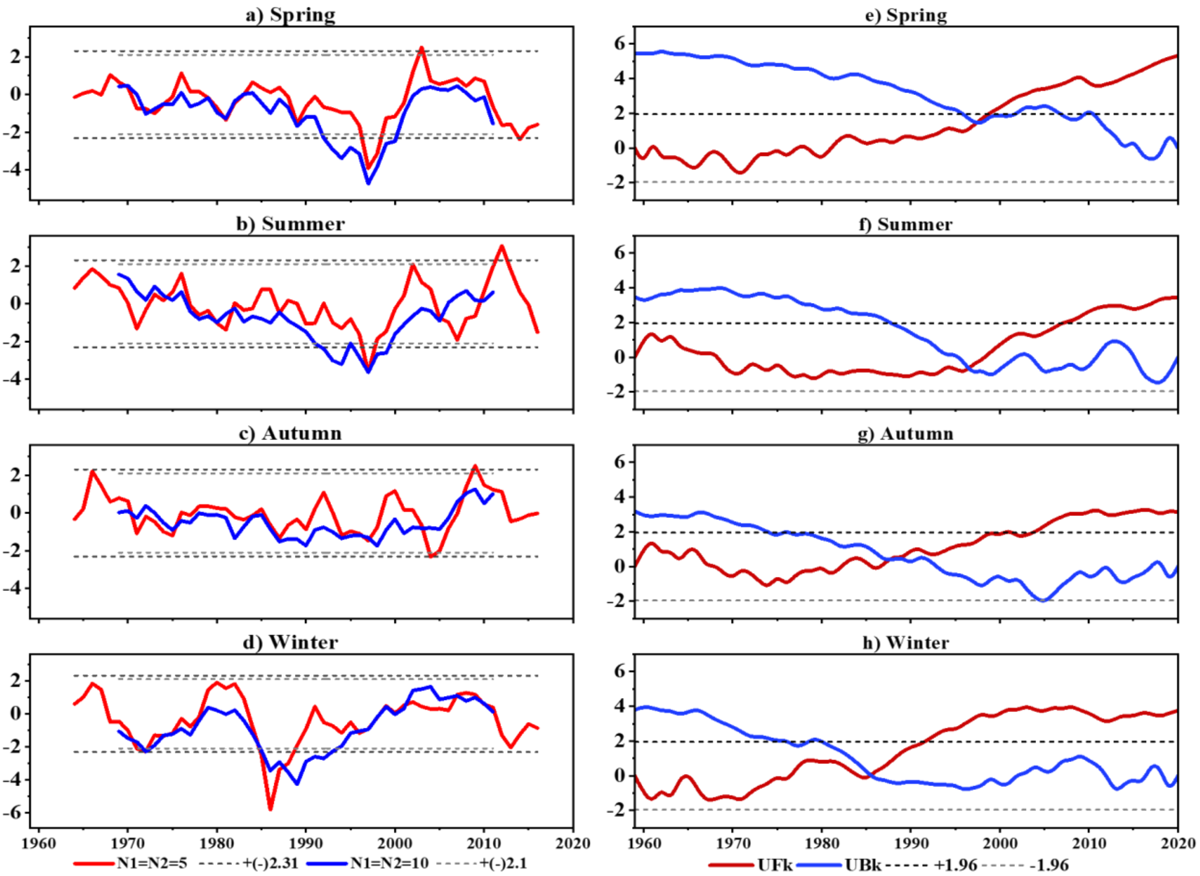

The results of the MTT and MK tests for the Yongding River Basin's annual temperature from 1959 to 2020 were displayed in Fig. 8.

Figure 8. Moving t-test (a) and Mann-Kendell mutation test (b) of annual temperature.

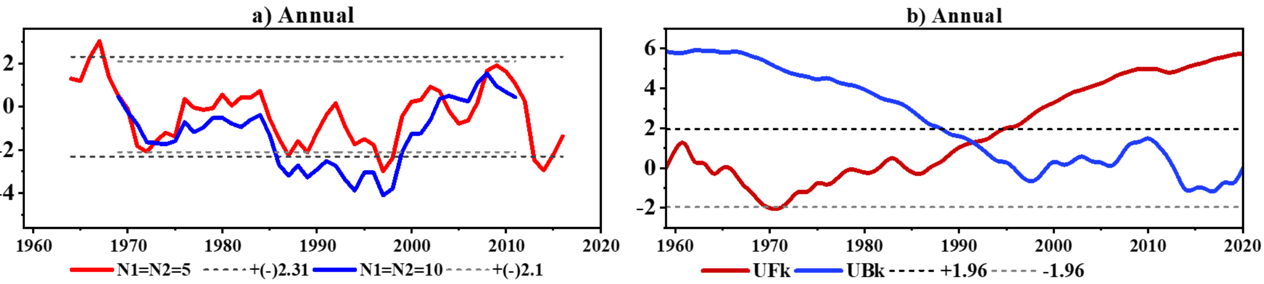

The computed annual temperature jumps between the two methods exhibit a slight discrepancy. In the MTT method (N1 = N2 = 5), three climate jumps (1967, 1997-1998, and 2013-2014) were observed, while in (N1 =

N2 = 10), only one jump (1986–1998) was identified. In contrast, the MK method showed only one jump (1992). The temperature jumps in the Yongding River Basin from 1959-2020 are presented in Table 4.

Table 4. Temperature jumps were detected by using MTT and MK methods in the Yongding River Basin from 1959-2020.

Time	**MTT**		**MK**
	N = 5	**N = 10**	
Spring	1997-1998, 2003, 2014	1992-2000	1997
Summer	1997, 2012	1992-1994, 1996-1999	1997
Autumn	2004, 2009	-	1988-1989
Winter	1986-1988, 2014	1972, 1985-1993	1986
Annual	1967, 1997-1998, 2013-2014	1986-1998	1992

Mean spring precipitation increased from 1961 to 1971, while decreased from 1972 to 1978, and increased again in 1979 to 2020. There was a significant increase observed from 2007 to 2020, while summer mean precipitation decreased from 1959 to 1968. It then experienced an increase from 1969 to 1982, followed by another decrease from 1983 to 2020. . There was a significant decrease noted from 2009 to 2020. Autumn mean precipitation exhibited a decrease from 1962 to 2007, followed by an increase from 2008 to 2020, with no significant overall trend. Winter mean precipitation decreased from 1962 to 1969 and increased from 1970 to 2020. Notably, significant increases were observed in 2016 and 2019.

The results of the MTT and MK tests for the seasonal precipitation in the Yongding River Basin from 1959 to 2020 were shown in Fig. 9. The Yongding River Basin seasonal precipitation MTT and MK test results from the study period of 1959 to 2020 revealed that the jump timings were not nearly consistent between the two these two methods MTT and MK. In the Yongding River Basin from 1959 to 2020, precipitation jumps were identified using the MTT and MK techniques, as shown in Table 5.

Table 5. Precipitation jumps were detected by using MTT and MK methods in the Yongding River Basin from 1959-2020.

Time	**MTT**		**MK**
	N1 = N2 = 5	**N1 = N2 = 10**	
Spring	1976, 1992	1978, 1982	1988, 1992, 1996
Summer	1997, 1999	1997, 2011	1982
Autumn	1989	1978 - 1979, 2007 - 2008	2007
Winter	-	-	1977, 1982 - 1983
Annual	1980	2010 - 2011	2015-2017,

Spatial Distribution of Temperature and Precipitation Jumps

In this study, the climate jump was considered in two parts: temperature and precipitation.

When examining the spatial distribution of temperature jumps, it is evident that multiple temperature jumps occurred in most areas of the Yongding River Basin (Figure 11).

The spatial distribution of spring mean temperature jumps is relatively simple, with one jump observed in the western and eastern parts of the study area (Shuozhou, part of Datong City, south of Zhangjiakou City), as well as in the Tianjin area, while no jumps occurred in other areas. For summer mean temperature jumps, most areas experienced a single jump, except for the downstream area of Guanting Reservoir. Regarding autumn mean

ISSN No. 2454-6194 | DOI: 10.51584/IJRIAS |Volume X Issue X October 2025

temperature jumps, two jumps occurred in Datong City and some areas in the northern part of Zhangjiakou City, while one jump occurred in the upper reaches of the Yongding River watershed, excluding these areas. In winter, temperature jumps occurred once in most of the study area. The area where a single temperature jump occurred in both summer and winter accounted for more than 94.09% of the area, which was found to have a significant impact on the annual average temperature jump. Table 6 presents the area percentage according to the number of jumps in annual and seasonal temperatures.

Figure 11. Spatial distribution of temperature jump throughout Yongding River basin between 1959 and 2020 (a) annual (b) spring (c) summer (d) autumn and (e) winter

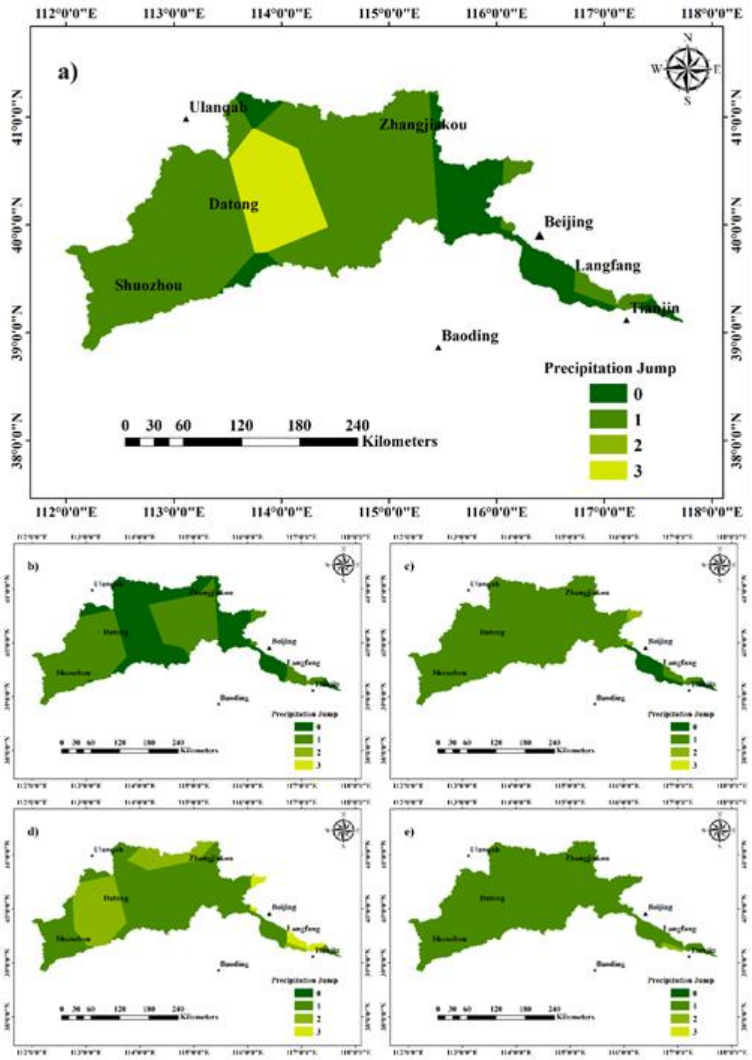

In the annual series, the area where temperature jumps occurred three times accounted for 12.9% of the total Yongding River Basin, while jumps occurred once in 71.07% of the area, and no jumps occurred in 16.03% of the area.

The spatial distribution of annual mean temperature jumps reveals three jumps in the central part of the study area (eastern part of Datong City) and one jump in the remaining area, except for some areas in the eastern and central parts where no jumps occurred.

Table 6. Area percentage according to the number of jumps of the annual and seasonal temperature.

Count	0	1	2	3
Annual	16.03	71.07	-	12.90
Spring	44.80	55.20	-	-
Summer	4.87	94.09	1.03	-
Autumn	-	69.67	27.45	2.89
Winter	-	99.36	0.64	-

INTERNATIONAL JOURNAL OF RESEARCH AND INNOVATION IN APPLIED SCIENCE (IJRIAS)
ISSN No. 2454-6194 | DOI: 10.51584/IJRIAS |Volume X Issue X October 2025

The precipitation jump is relatively complicated as compared to the temperature jump as shown in (Fig. 12). The spatial distribution of spring mean precipitation jumps is diverse, with three jumps occurring in the northern part of Zhangjiakou City and the southern part of Datong City, two jumps in the southern part of Zhangjiakou City and around Beijing, and one jump in the western part of the study area and the Guanting Reservoir outflow area. Small areas in the northern, south-central, and eastern parts of the study area did not experience any jumps. In most areas, the range of summer mean annual precipitation jumps was from one to two, with a very small area experiencing three jumps. Autumn mean precipitation jumps occurred three times in the north-central and south-central parts of the study area, and one or two times in the remaining area. In winter, mean precipitation jumps did not occur in Zhangjiakou City, the lower reaches of Yanghe, Sangganhe, and Guanting Reservoir, while one or two jumps occurred in other areas.

Figure 12. Spatial distribution of precipitation jumps throughout Yongding River basin between 1959 and 2020 (a) annual (b) spring (c) summer (d) autumn and (e) winter

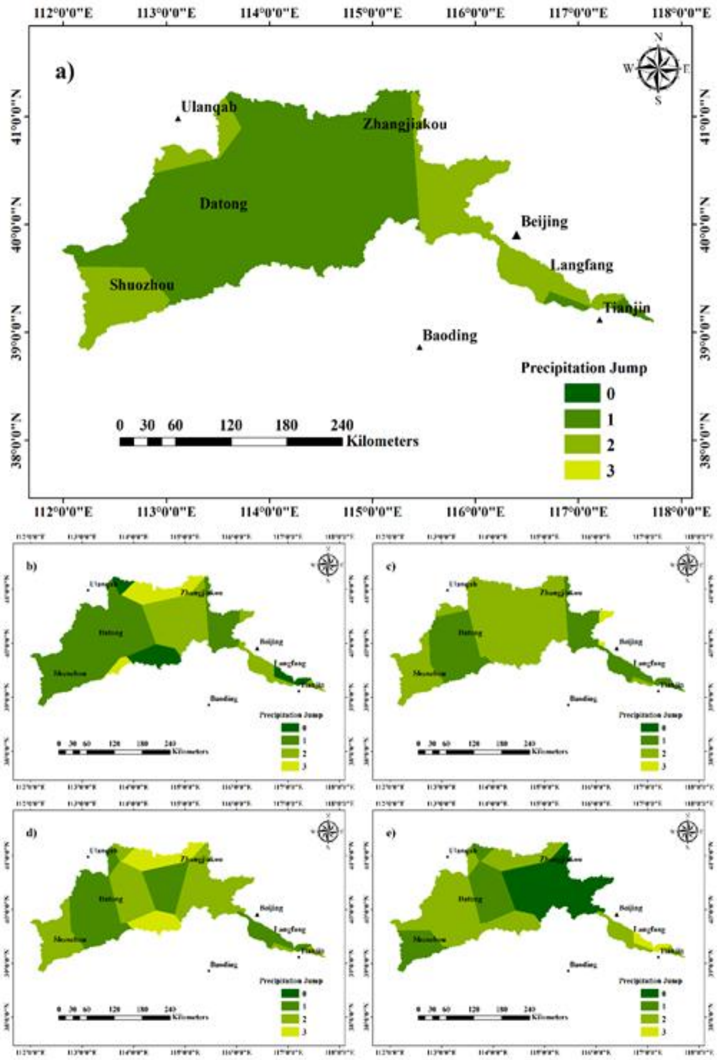

The areas where climate jumps did not occur in spring and winter account for 8.92% and 29.96% of the total Yongding River Basin, respectively. However, the impact on the total precipitation jumps is not as significant since the precipitation is relatively low during these seasons. In summer and autumn, more than one precipitation jump occurred in all areas.

Table 7. Area percentage according to the number of jumps of the annual and seasonal precipitation

Count	0	1	2	3
Annual	-	73.87	26.13	-
Spring	8.92	55.69	26.44	8.95
Summer	-	35.22	63.75	1.03

Autumn	-	39.98	46.77	13.25
Winter	29.96	22.50	45.68	1.85

The spatial distribution of annual mean precipitation jumps reveals that most areas in the central part of the study area (Datong City and Zhangjiakou City) experienced one jump, while most areas around Shuozhou City and the eastern part of the study area had two jumps. In the annual series, the area where the average annual precipitation jump occurred once accounted for 73.87% of the total watershed area, and the area where the jump occurred twice accounted for 26.13%, with no area experiencing no jump. This indicates that the main cause of the annual precipitation jump is the change in precipitation during summer and autumn, which exhibits high variability and severity in this basin.

The duration of historical data makes it difficult to identify variations in temperature and precipitation. On the other hand, this is a characteristic that many people have, and multi-time scale characteristics can be found in both seasonal and annual precipitation. The results vary depending on the area characteristics and the time period of selected historical data; some are obvious while others are not.

Analysis of Annual Precipitation and Temperature

In accordance with the results of the Mann-Kendall test, which used annual average temperature data from 1959 to 2020, the average annual temperature at 53 stations (i.e., 100% of the total number of stations) shows an upward trend, with the trend toward growth being significant at every station. No station, however, displays a downward trend. The yearly average temperature in China has increased significantly over the past 48 years, according to analyses conducted by other researchers [36]. The overall warming trend in China's climate by analyzing meteorological data from 1950 to 2010 [37]. According to [38], there has been a significant increase in the annual mean minimum, mean, and maximum temperatures in northeast China, each by around 2.11°C, 1.59°C, and 1.13°C, respectively [39].

As per Mann-Kendall test results on annual precipitation changes from 1959 to 2020, 25 stations showed a decreasing trend, while 28 stations showed an increasing trend. The annual mean precipitation in the Yongding River Basin decreased during the study period, with annual and summer precipitation rates decreasing by -0.053 mm a-2 and -0.75 mm season-1 a-1, respectively. Since the 1960s, the Wei River basin's average annual precipitation has been decreasing, by about 2 mm every 10 years. The Mudanjiang River Basin, the higher sections of the Xiliao River, and the lower reaches of the Songhua River all experienced an increase or strengthening in frequency and intensity [40].

Analysis of Seasonal Precipitation and Temperature

The results of the Mann-Kendall test revealed that there was an increasing trend in the average spring and summer temperatures of the various regions in the Yongding River Basin from 1959 to 2020 at all of the selected stations, and that this increasing trend was significant at each station.

At each station, the average autumn temperature shows an increasing trend. Of these, 48 stations had considerable increases in the trend, which was characterized by abrupt changes. According to Sulikowska's research, the pace of change during the last 40 years has been more than three times that of the entire study period, indicating that the trend toward high temperatures is accelerating. Summer in Central and Eastern Europe has changed the most during the past 40 years [40]. The autumn and winter rainfall is on a declining trend, whereas summer rainfall is on the rising trend. According to the findings, there was a positive trend in the late spring and summer due to an increase in minimum temperatures, and a negative trend in the autumn and winter due to a decrease in maximum temperatures [41].

All sites displayed an increasing trend for the average spring and winter temperature, which was significant at 49 stations. Some eastern regions experienced notable changes in precipitation patterns during the spring. There were noticeable changes in precipitation patterns during the spring in several eastern locations. All areas of the Yongding River Basin experienced less precipitation during the summer. Precipitation increased in parts of all regions of the river basin in autumn, but the change was not significant. The east and west regions of the Yongding River Basin showed significant differences in winter precipitation.

Correlation Analysis between mean temperature and precipitation

In Yongding River Basin 46 stations, (i.e., 86.8% of all the selected stations) showed negative correlations between annual mean temperature and annual precipitation, with almost all of these stations showing weak and low negative correlations. In the Yongding River Basin, 46 stations (or 86.8% of the stations chosen) displayed negative correlations between annual mean temperature and yearly precipitation. Nearly all of these stations displayed weak and low negative correlations.

In the Yongding River Basin, average temperatures and precipitation were typically found to be negatively correlated, but the values varied greatly by season. The arid region experiences the strongest link between temperature and precipitation. The ecological security of the arid zone is threatened by the dry zone's fragile state, changes in precipitation quantity, and aggravated by temperature variations. The relationship in the semi-humid zone may be more complex as a result of the monsoon's influence on the overall amount of precipitation and temperature. However, in the dry and semi-arid zones, temperature variations have a similar effect on precipitation quality [42].

Climate jumps detection during 1959-2020

Summer precipitation accounted for 65.8% of annual precipitation, with a standard error being high in months with high precipitation. August had the greatest trend (-1.13 mm month-1 a-1) followed by July (-0.71 mm month-1 a-1). This measurement was supported by the cumulative precipitation anomaly, as both annual and summer precipitation rates decreased. The rainfall pattern in Madagascar reflects the effects of global warming, with annual rainfall rising as temperatures and elevations rise. However, irrespective of height, the yearly rainfall increases if the annual temperature rises by more than 0.03 °C [43]. The trend toward drought and extreme heat in Europe have been investigated, and it is mostly driven by the trend toward decreased total precipitation, with the trend toward increased temperature having a minimal direct impact [44].

CONCLUSIONS

The Yongding River Basin's temperature and precipitation trends, as well as their significance, were investigated in this study using the Mann-Kendall test. Spearman's correlation analysis was also performed to assess the degree of association between these two climate parameters, and the moving t-test was employed to identify climate leaps.

In summary, 100% of the stations under examination showed a significant upward trend, which was more pronounced in the spring than in other seasons. The annual and seasonal mean temperature in the Yongding River Basin has an upward tendency. However, the Yongding River Basin's eastern and western sections showed high consistency with inter-annual and inter-seasonal variations, with a considerable increasing tendency, which had an impact on the degree of temperature changes. Notwithstanding slightly similar results in other areas of the Yongding River Basin, the general trend of rising temperatures was still discernible. Although there has been an overall drop in annual precipitation in the Yongding River Basin, there have been certain regions where it has increased. The stations with expanding trends were generally in the various regions of the Yongding River Basin, with an increasing trend in total precipitation that changed in the spring and a more convoluted increasing trend in total precipitation corresponding to different seasons. Whereas the variances in the overall amount of precipitation declined during the winter and autumn seasons.

Spearman's correlation analysis was used to find the correlation between mean temperature and precipitation at both the inter-annual and inter-seasonal scales. At both the inter-annual and inter-seasonal timeframes, the connection between temperature and precipitation in the Yongding River Basin was unfavorable. Evidently, 46 stations displayed negative correlations between annual mean temperature and yearly mean precipitation, with 33 and 11 stations exhibiting flimsy and low negative correlations, respectively. Precipitation and annual mean temperature did not generally correlate well. The variation of climate change was determined using the moving t-test, with 84.9% (45 out of 53 metrological stations) and 90.6% (48 out of 53 stations) of the stations identifying climatic leaps for the summer series and annual series, respectively. There was the same number of metrological sites for both the annual and summer series where a single climate fluctuation was noted.

ACKNOWLEDGEMENTS

We thank to all researchers of Faculty of Geoscience and Technology of Kim Chaek University of Technology, who gave us useful assistance and support.

Compliance With Ethical Standards

Conflict of Interest

The authors have no competing interests to declare that are relevant to the content of this article.

Author Contributions

Hui Gwang Yun - Investigation, Writing-Original Draft (*e-mail address: yhg8439@star-co.net.kp)

Il Chol Kim - Project Administration, Conceptualization (kic2003718@star-co.net.kp)

Kwang Jin Rim - Software (rkj96819@star-co.net.kp)

Chol Ho Chae - Methodology (cch5738@star-co.net.kp)

REFERENCES

1. ZHANG, L., CHEN, X., ZHAO, Z. & HU, Z. 2008a. Progress in study of climate change impacts on hydrology and water resources [J]. Progress in Geography, 3.
2. CHANGE, C. 2013. IPCC, The Physical Science Basis Summary for Policymakers, Technical Summary and Frequently Asked Questions.
3. DORE, M. H. 2005. Climate change and changes in global precipitation patterns: what do we know? Environment international, 31, 1167-1181.
4. HSU, P. C., LI, T. & WANG, B. 2011. Trends in global monsoon area and precipitation over the past 30 years. Geophysical Research Letters, 38.
5. GREVE, P., ORLOWSKY, B., MUELLER, B., SHEFFIELD, J., REICHSTEIN, M. & SENEVIRATNE, S. I. 2014. Global assessment of trends in wetting and drying over land. Nature geoscience, 7, 716-721.
6. MIAO, C. Y., DUAN, Q. Y., SUN, Q. H., LEI, X. H. & LI, H. 2019. Non-uniform changes in different categories of precipitation intensity across China and the associated large-scale circulations. Environmental Research Letters, 14, 025004.
7. PIAO, S., CIAIS, P., HUANG, Y., SHEN, Z., PENG, S., LI, J., ZHOU, L., LIU, H., MA, Y. & DING, Y. 2010. The impacts of climate change on water resources and agriculture in China. Nature, 467, 43-51.
8. FIELD, C. B., BARROS, V., STOCKER, T. F. & DAHE, Q. 2012. Managing the risks of extreme events and disasters to advance climate change adaptation: special report of the intergovernmental panel on climate change, Cambridge University Press.
9. ZHAN, Y. J., REN, G. Y. & YANG, S. 2018. Change in precipitation over the Asian continent from 1901-2016 based on a new multi-source dataset. Climate Research, 76, 41-57.
10. WANG, H. J. & CHEN, H. P. 2012a. Climate control for southeastern China moisture and precipitation: Indian or East Asian monsoon? Journal of Geophysical Research-Atmospheres, 117.
11. LIU, B., YAN, Z. H., SHA, J. X. & LI, S. 2017. Drought Evolution Due to Climate Change and Links to Precipitation Intensity in the Haihe River Basin. Water, 9, 878.
12. YAN, Z. H., WANG, S. Q., MA, D., LIU, B., LIN, H. & LI, S. 2019. Meteorological Factors Affecting Pan Evaporation in the Haihe River Basin, China. Water, 11, 317.
13. SUN, Y., LIU, Q., LI, Q. & YUAN, X. 2019. Temporal Variation of Precipitation Characteristics in Haihe Basin during Recent 60 Years. Journal of Water Resources Research, 8, 117-124.
14. YU, Y., YANG, Z., LIU, Y., QIN, D. & LIU, J. 2010. Review of study on precipitation of Haihe River Basin under changing environment. Journal of China Hydrology, 30, 32-35.
15. DAI, D., SUN, M., LV, X., HU, J., ZHANG, H., XU, X. & LEI, K. 2022. Comprehensive assessment of the water environment carrying capacity based on the spatial system dynamics model, a case study of Yongding River Basin in North China. Journal of Cleaner Production, 344, 131137.

16. YI, Z., SONG, Z., YANG, R., LE, Z., LI, X. & SUN, M. 2019. Design of Data Acquisition Scheme for Cross-boundary Section Based on Wireless Sensor Network: A Case Study of Guanting Reservoir in Yongding River Basin. Proceedings of the 7th International Conference on Communications and Broadband Networking. Nagoya, Japan: Association for Computing Machinery.
17. LU, Y., WU, B., YAN, N., ZENG, H., GUO, Y., ZHU, W. & ZHANG, H. 2021. Method for monitoring environmental flows with high spatial and temporal resolution satellite data. Environmental Monitoring and Assessment, 194, 13.
18. WANG, M., DU, L., KE, Y., HUANG, M., ZHANG, J., ZHAO, Y., LI, X. & GONG, H. 2019. Impact of Climate Variabilities and Human Activities on Surface Water Extents in Reservoirs of Yongding River Basin, China, from 1985 to 2016 Based on Landsat Observations and Time Series Analysis. 11, 560.
19. WANG, L., WANG, Z. J., KOIKE, T., YIN, H., YANG, D. W. & HE, S. 2010. The assessment of surface water resources for the semi-arid Yongding River Basin from 1956 to 2000 and the impact of land use change. Hydrological Processes, 24, 1123-1132.
20. PAN, T., ZUO, L., ZHANG, Z., ZHAO, X., SUN, F., ZHU, Z. & LIU, Y. 2021. Impact of Land Use Change on Water Conservation: A Case Study of Zhangjiakou in Yongding River. 13, 22.
21. LU, S., ZHANG, L., GUO, S., FAN, L., MENG, J. & WANG, G. 2016. Forty years' channel change on the Yongdinghe River, China: patterns and causes. International Journal of River Basin Management, 14, 183-193.
22. Akgül, M. A., & Aksu, H. 2021. Areal Precipitation Estimation Using Satellite Derived Rainfall Data over an Irrigation Area. Turkish Journal of Agriculture-Food Science and Technology, 9(2), 386-394. https://doi.org/doi.org/10.24925/turjaf.v9i2.386-394.4061
23. Saedi, J., Sharifi, M. R., Saremi, A., & Babazadeh, H. (2022). Assessing the impact of climate change and human activity on streamflow in a semiarid basin using precipitation and baseflow analysis. Scientific Reports, 12(1), 9228.
24. FAISAL, N. & GAFFAR, A. 2012. Development of Pakistan's new area weighted rainfall using Thiessen polygon method. Pakistan Journal of Meteorology (Pakistan).
25. DUMAN, E. & KARA, F. 2017. A Study on Trends and Variability in Monthly Temperatures in Antalya Province between the Years 1960 and 2015. Journal of Scientific Research & Reports, 14, 1-16.
26. TUFA, G. K. & MEGARSA, E. S. 2021. Evaluation of Variability of Watershed Hydrological Partitioning: The Case of Mormora River, South Eastern Ethiopia. Journal of Water Resources and Ocean Science, 10, 132-138.
27. ZUBAIRU, M. S., ASIEDU, W. L. A. G. M., LASHARI, K. A. H. J. J. O. A. S. R. & VOLUME 2021. The Impact of Climate Change on Rainfall Patterns in Ghana: A Zon-ing Adaptation Strategy through Developing Agroforestry. 4
28. CHU, J., XIA, J., XU, C., LI, L. & WANG, Z. 2010. Spatial and temporal variability of daily precipitation in Haihe River basin, 1958–2007. Journal of Geographical Sciences, 20, 248-260.
29. HAN, Y., LIU, B., XU, D., YUAN, C., XU, Y., SHA, J., LI, S., CHANG, Y., SUN, B. & XU, Z. 2021. Temporal and Spatial Variation Characteristics of Precipitation in the Haihe River Basin under the Influence of Climate Change. Water, 13, 1664.
30. WANG, L., ZHU, H., LU, F. & HE, L.-X. 2012b. Characteristics of temporal and spatial variation of precipitation in Haihe River Basin during recent 50 years. Agricultural Research in the Arid Areas, 30, 242-246.
31. LI, Z. & JIANG, F. 2007. A study of abrupt climate change in Xinjiang region during 1961–2004. Journal of Glaciology and Geocryology, 29, 351-359.
32. LIANG, L., LI, L. & LIU, Q. 2010. Temporal variation of reference evapotranspiration during 1961–2005 in the Taoer River basin of Northeast China. Agricultural and Forest Meteorology, 150, 298-306.
33. LIANG, L., LI, L. & LIU, Q. 2011. Precipitation variability in Northeast China from 1961 to 2008. Journal of Hydrology, 404, 67-76.
34. LV, X., ZUO, Z., NI, Y., SUN, J. & WANG, H. J. S. R. 2019. The effects of climate and catchment characteristic change on streamflow in a typical tributary of the Yellow River. 9, 1-10.
35. Yan, M., Deng, W., & Chen, P. 2003. Recent trends of temperature and precipitation disturbed by large-scale reclamation in the Sangjiang plain of china. Chinese Geographical Science, 13(4), 317-321. https://doi.org/10.1007/s11769-003-0036-1

36. MA, Z., GUO, Q., YANG, F., CHEN, H., LI, W., LIN, L. & ZHENG, C. 2021. Recent Changes in Temperature and Precipitation of the Summer and Autumn Seasons over Fujian Province, China. Water, 13, 1900.
37. HUANG, W., YANG, J., LIU, Y. & YU, E. 2021. Spatiotemporal Variations of Drought in the Arid Region of Northwestern China during 1950–2012. Advances in Meteorology, 2021.
38. HU, Z. Z., YANG, S. & WU, R. 2003. Long-term climate variations in China and global warming signals. Journal of Geophysical Research: Atmospheres, 108.
39. ZHANG, H., CHEN, Y., REN, G. & YANG, G. 2008b. The characteristics of precipitation variation of Weihe River Basin in Shaanxi Province during recent 50 years. Agricultural Research in the Arid Areas, 26, 236-242.
40. SULIKOWSKA, A. & WYPYCH, A. 2021. Seasonal Variability of Trends in Regional Hot and Warm Temperature Extremes in Europe. Atmosphere, 12, 612.
41. CALOIERO, T., BUTTAFUOCO, G., COSCARELLI, R. & FERRARI, E. 2015. Spatial and temporal characterization of climate at regional scale using homogeneous monthly precipitation and air temperature data: an application in Calabria (southern Italy). Hydrology Research, 46, 629-646.
42. HUANG, Y., CAI, J., YIN, H. & CAI, M. 2009. Correlation of precipitation to temperature variation in the Huanghe River (Yellow River) basin during 1957–2006. Journal of Hydrology, 372, 1-8.
43. OGURTSOV, M. 2021. Decadal and Bi-Decadal Periodicities in Temperature of Southern Scandinavia: Manifestations of Natural Variability or Climatic Response to Solar Cycles? Atmosphere, 12, 676.
44. BEZAK, N. & MIKOŠ, M. 2020. Changes in the compound drought and extreme heat occurrence in the 1961–2018 period at the European scale. Water, 12, 3543.